Microbial Pathogenesis 199 (2025) 107252

Contents lists available at ScienceDirect

Microbial Pathogenesis

journal homepage: www.elsevier.com/locate/micpath

Upregulation of haematopoetic cell kinase (Hck) activity by a secreted parasite effector protein (Ta9) drives proliferation of *Theileria annulata*-transformed leukocytes

Shahin Tajeri [a,b,*], Brian Shiels [c], Gordon Langsley [d,e], Ard Menzo Nijhof [a,b,**]

[a] Freie Universität Berlin, Institute for Parasitology and Tropical Veterinary Medicine, Berlin, Germany
[b] Freie Universität Berlin, Veterinary Centre for Resistance Research, Berlin, Germany
[c] School of Biodiversity, One Health and Veterinary Medicine, College of Medical, Veterinary and Life Sciences, University of Glasgow, Glasgow, United Kingdom
[d] Inserm U1016-CNRS UMR8104, Institut Cochin, Paris, France
[e] Laboratoire de Biologie Comparative des Apicomplexes, Faculté de Médecine, Université Paris Descartes - Sorbonne Paris Cité, Paris, France

ARTICLE INFO

Keywords:
Theileria annulata
Ta9
Leukocyte transformation
gene expression
Hematopoietic cell kinase (HCK)

ABSTRACT

Reversible transformation of bovine leukocytes by the intracellular parasites *Theileria annulata* and *Theileria parva* is central to pathogenesis of the diseases they cause, tropical theileriosis and East Coast Fever, respectively. Parasite-dependent constitutive activation of major host transcription factors such as AP-1 (Activating Protein 1) and NF-κB (Nuclear Factor-Kappa B) sustains the transformed state. Although parasite interaction with host cell signaling pathways upstream of AP-1 have been studied, the precise contribution of *Theileria* encoded factors capable of modulating AP-1 transcriptional activity, and other infection-altered signaling pathways is not fully understood. We previously showed that the Ta9 protein from *T. annulata* (TA15705) is secreted into the host cell cytoplasm and contributes to infection-induced AP-1 transcriptional activity. The current study employed RNA-seq to investigate the ability of ectopically expressed Ta9 to modulate the gene transcription profile of a bovine macrophage cell line, BoMac. RNA-seq identified 560 (400 upregulated and 160 downregulated) differentially expressed genes. KEGG analysis predicted a high number of upregulated genes associated with carcinogenesis such as *CCND1*, *CDKN1A*, *ETV4*, *ETV5*, *FLI1*, *FRA1*, *GLI2*, *GRO1*, *HCK*, *IL7R*, *MYBL1*, *MYCN*, *PIM1* and *TAL1*. Ta9 introduction also affected genes associated with proinflammatory processes such as cytokines, chemokines, growth factors and metalloproteinases. Enrichment analysis of differentially expressed genes revealed that Ta9 is potentially involved in activating other host cell signaling pathways in addition to those that lead to induction of AP-1. Comparing our data with data on differentially expressed BoMac genes modulated by the secreted TashAT2 factor of *T. annulata* identified the gene encoding the tyrosine protein kinase hematopoietic cell kinase (HCK) as common to both data sets. HCK is essential for the proliferation of *T. parva*-transformed B cells and herein, we demonstrate that enzymatic activity of HCK is also essential for *T. annulata*- and *T. lestoquardi*-transformed macrophage proliferation.

1. Introduction

Theileria parasites belong to the phylum Apicomplexa and are closely related to *Plasmodium* parasites, the causal agent of malaria in humans and animals. However, unlike the mosquito-borne *Plasmodium* spp., *Theileria* parasites are tick transmitted. Transstadially-infected nymph or adult ticks inject sporozoites (the parasite stage infective for the vertebrate host in all Apicomplexans) when feeding on new hosts that include mammals of the bovidae, ovidae and equidae families. *Theileria* sporozoites randomly come into contact with leukocytes that reside in tissues proximate to the tick attachment site. They quickly invade B cells and T cells (*T. parva*) or B cells and myeloid cells (*T. annulata*) in which they replicate by schizogony. Transforming *Theileria* species schizonts provoke the uncontrolled proliferation and immortalization of infected leukocytes [1]. Coincident to this, the parasite population is also amplified, as during leukocyte cell division schizonts are partitioned

* Corresponding author. Freie Universität Berlin, Institute for Parasitology and Tropical Veterinary Medicine, Berlin, Germany.
** Corresponding author. Freie Universität Berlin, Institute for Parasitology and Tropical Veterinary Medicine, Berlin, Germany.
E-mail addresses: shahin.tajeri@fu-berlin.de (S. Tajeri), ard.nijhof@fu-berlin.de (A.M. Nijhof).

https://doi.org/10.1016/j.micpath.2024.107252
Received 7 August 2024; Received in revised form 9 December 2024; Accepted 20 December 2024
Available online 25 December 2024

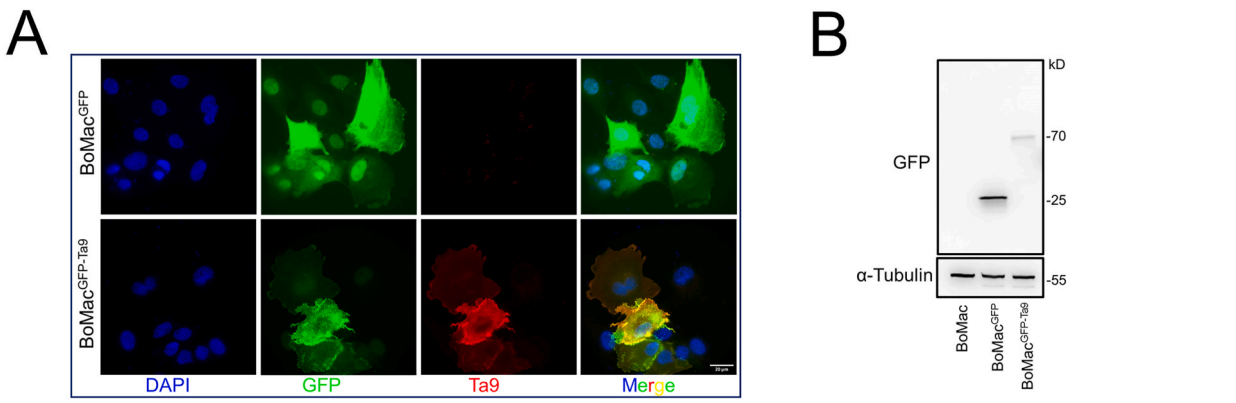

Fig. 1. Confirmation of GFP expression in BoMac^{GFP} and BoMac$^{GFP-Ta9}$ cells. **A**, Bovine macrophages (BoMac) stably expressing GFP, or GFP-Ta9 were grown and fixed on coverslips. Expression of GFP in both cell lines was confirmed by immunofluorescent microscopy to reveal a cytoplasmic and membrane associated pattern for GFP-Ta9 that was distinct from the diffuse cytoplasmic and nuclear GFP pattern. The cells were also stained with a rat anti-Ta9 serum (shown in red) to further confirm high to lower level Ta9 expression only in BoMac$^{GFP-Ta9}$, and not in BoMac^{GFP} cells. Bar = 20 μm. **B**, Western blot of protein extracts prepared from BoMac^{GFP} and BoMac$^{GFP-Ta9}$ cells to estimate overall GFP expression in both groups. Expression of the 70 kDa Ta9-GFP protein was detectably lower compared to 25 kDa GFP in the transfected bovine macrophages. Anti-Tubulin antibody was used as a loading control.

into each daughter cell by tightly anchoring to the host mitotic spindle [2]. During the course of infection, an unknown stimulus provokes schizonts to develop into merozoites that once released from the ruptured leukocyte invade red blood cells that can be ingested by ticks, in which sexual reproduction and sporogony occurs. The three major transforming species are *T. parva* and *T. annulata* in cattle and *T. lestoquardi* in sheep and goats: the lymphoproliferative diseases they cause (East Coast Fever, tropical theileriosis, and malignant ovine theileriosis, respectively) are frequently fatal and a significant economic burden in endemic areas such as Asia, the Middle East and Africa [3,4].

Theileria-induced leukocyte transformation results from a complex crosstalk between host and parasite [5,6]. Many cellular and molecular changes occur in transformed leukocytes and have been well documented [7,8]; notable examples include constitutive activation of key host cell transcription factors such as AP-1 [9,10], NF-κB [11,12], Hypoxia inducible factor 1α (HIF1α) [13,14] and c-MYC [15]. This activation results in substantial changes to mRNA and microRNA expression profiles of infected versus non-infected leukocytes, with expression of more than 1000 host genes being increased or decreased following infection [16–21]. Several host kinases (JNK, Src and IKKs) upstream of these transcription factors have been identified, as being constitutively activated by live parasites [10,22–27]. For example, tyrosine kinases of the Src family have been shown to be essential for proliferation of *T. parva*-transformed cells [22,23]. Hematopoietic Cell Kinase (HCK) is specifically expressed by cells of the hematopoietic lineage [28]. In *T. parva*-transformed B lymphocytes, HCK is constitutively active due to infection-induced exclusion of the Src inhibitor C-terminal Src kinase (CSK) from lipid rafts, where HCK is located [22]. Active HCK contributes to both AP-1-driven transcription [22] and in *T. annulata*-transformed macrophages it also contributes to modulation of actin dynamics [29,30].

Theileria, unlike *Plasmodium* and *Toxoplasma,* does not reside within a parasitophorous vacuole, meaning that secreted *Theileria* proteins can be delivered directly into the cytosol of infected leukocytes to interact with host cell proteins. Bioinformatic analysis of the *T. annulata* genome identified 3250 genes [31]. Of these, 1197 are expressed in schizonts and 167 (14 %) were predicted to encode a signal peptide to allow secretion; reviewed in Ref. [32]. The parasite therefore has the potential to secrete a large number of putative effector proteins into the host cell cytosol [33]. One putative secreted effector protein is Ta9 (encoded by TA15705) that was originally identified as a highly dominant parasite antigen recognized by protective bovine CD8 T cells [34], and subsequently shown to sustain AP-1-driven transcription [35]. The cytosolic localization of Ta9 was recently characterized as a member of the exportome of secreted intrinsically disordered proteins and its cytosol location was validated [36].

In this study we undertook further characterization of Ta9 as a critical parasite effector of host cell transformation because: 1) Ta9 does not possess any orthologue in non-transforming *T. orientalis*; 2) Ta9 is highly expressed in the cell-transforming schizont stage; 3) Ta9 expression goes down rapidly as host cell division subsides during differentiation of schizonts to non-transforming merozoites; 4) Ta9 protein is abundant in the host compartment of infected leukocytes; 5) Ta9 contributes to AP-1 activation, and sustained AP-1 activation is a hallmark of leukocytes transformed by *T. annulata* and *T. parva*. Our primary aim of this study was to examine whether secreted Ta9 can activate signaling pathways over and above those that lead to AP-1 induction. To this end, RNA-seq was performed on non-infected bovine macrophages (BoMac) that stably expressed a green fluorescent protein (GFP)-tagged version of Ta9 compared to BoMacs stably expressing the GFP tag alone. Expression of Ta9 clearly altered bovine macrophage gene expression, demonstrating that Ta9 has the potential to modulate a range of host cell signaling pathways. Moreover, we provide evidence that Ta9 can upregulate expression of the host proto-oncogene *hck* and show that heightened HCK activity is important for proliferation of both *T. annulata*- and *T. lestoquardi*-transformed macrophages.

2. Materials and methods

2.1. Cell culture and generation of stable GFP expressing bovine macrophages

SV40 virus transformed peritoneal bovine macrophages (BoMac) [37] were seeded in six well cell culture plates and were transfected (X-tremeGENE™ HP DNA transfection reagent, Roche) with 1 μg per well of plasmid DNA encoding GFP or GFP-tagged Ta9 [35], in separate plates, at 80 % confluency. Forty-eight hours post transfection cell supernatants were replaced with fresh medium containing 50 μg/μl hygromycin (Carl Roth, Germany, Art. No. 1287.1) as the selection drug. Hygromycin was refreshed every 72 h until non-GFP expressing cells were eliminated and clones emerged. The GFP expressing cells were then expanded and passaged in 25 μg/μl hygromycin for downstream experiments. BoMacs were cultured in commercial DMEM medium containing 15 mM HEPES and 2.5 mM L-glutamine (Cytiva HyClone™). Heat inactivated bovine serum (FBS, Gibco, Cat. No. A5670501) and penicillin-streptomycin (10000 U/ml, Gibco, Cat. No. 15140122) were added to the commercial medium to obtain a final concentration of 10 % FBS and 100 units per ml of antibiotics (peniciilin/streptomycin).

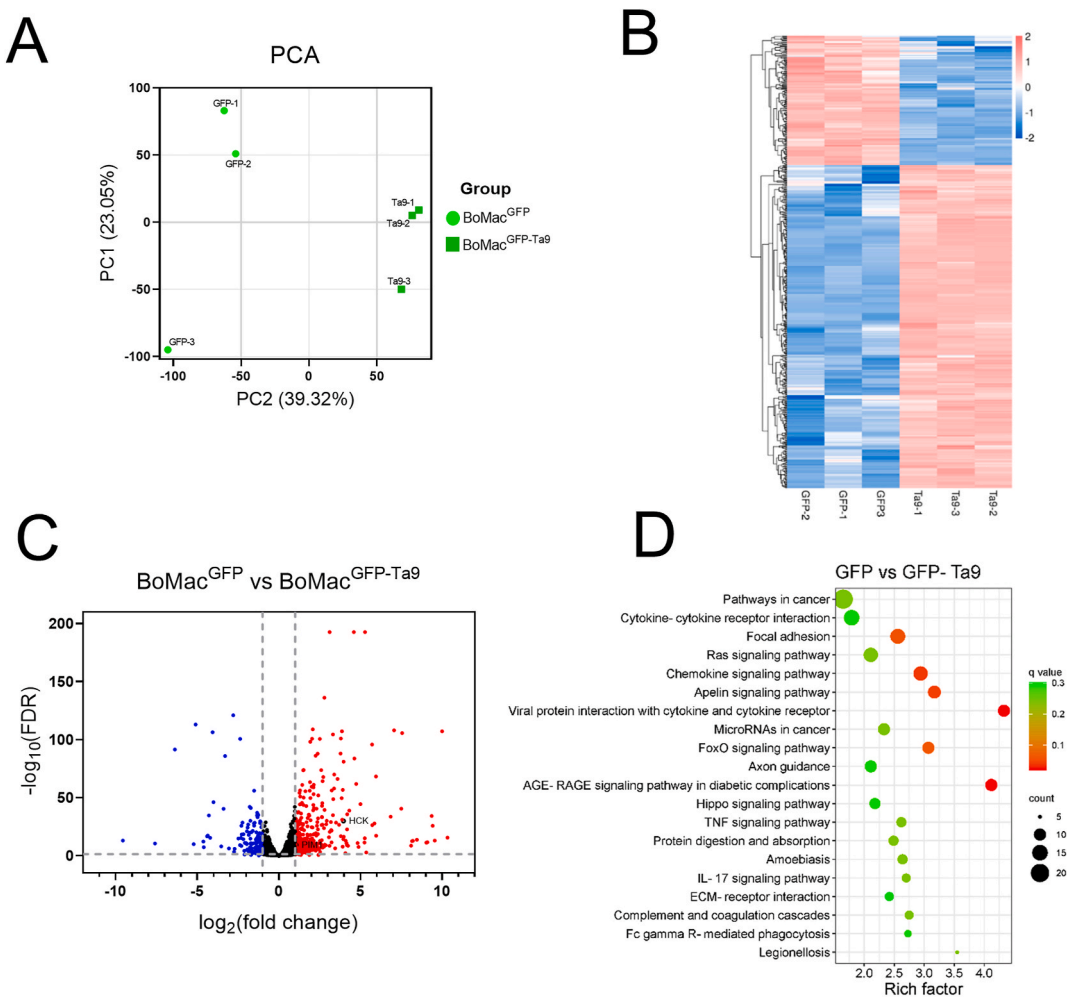

Fig. 2. RNA-seq analysis of the impact of Ta9 expression on bovine macrophage gene transcription. **A**, PCA (Principal Component Analysis) plot of GFP- and GFP-Ta9-expressing macrophages. PC1 and PC2 are two principal components, color intensity and shapes represent biological replicates for each cell line. **B**, Global changes and hierarchical clustering of Ta9-associated DEGs across replicate samples. Each column represents one sample and rows represent genes. Expression levels were visualized using a scale from least to most abundant ranging from −2.0 (dark blue) to 2.0 (dark red). The expression level of genes (FPKM) was normalized by log10, i.e. log10 (FPKM+0.000001). Expression relationships are shown on the left. The top tree indicates the cluster relationship of samples. **C**, Differential expression Volcano plot, where each dot represents a gene. X-axis: log2Fold change in expression; Y-axis: log10(FDR). Dots farther from y = 0 represent genes with large differences in expression between GFP- and GFP-Ta9-expressing bovine macrophages. Dots farther from x = 0 represent genes where the difference is more statistically reliable. Blue dots ($n = 160$) are relatively lower-expressed genes for the GFP-Ta9 line, while red dots ($n = 400$) are elevated expressed genes, black dots represent genes displaying no significant difference in expression. The Volcano plot was created with GraphPad Prism v8.4. **D**, A rich factor bubble plot depicting KEGG pathway enrichment of Ta9-associated DEGs. Each dot represents a KEGG pathway. Y-axis: Pathway; X-axis: Rich factor. Rich (Enrichment) factor is calculated as "Enrichment factor = (Ratio of DEGs annotated to the term over all DEGs)/(Ratio of genes annotated to the term over all genes)". A greater enrichment factor indicates a more significant enrichment of the pathway. The color of the dots stands for q-value (adjusted p-value). The smaller the q-value the more significant or reliable is the enrichment. The size of the dots represents the number of DEGs enriched in the pathway. The larger the dot is, the more genes it contains. Top 20 enriched pathways are shown. The plot was created with SRplot platform [80].

Theileria annulata transformed cell lines included TaC12 (macrophage) [2] and the clinical isolate Ankara [38]. *Theileria lestoquardi* (Atbara strain) transformed sheep leukocytes were isolated in Sudan and used at passage 60 [39]. Buparvaquone resistant TaC12 cells were as described [40]. All *Theileria* transformed cells were cultured in cultured in RPMI1640 + L-glutamine (Gibco™, Cat. No. 11875101) supplemented with 10 % fetal bovine serum (Gibco™), 10 mM HEPES (Carl Roth, Art. No. 9157.1), 100 U/ml penicillin/streptomycin (Gibco™) and passaged three times a week. In cell proliferation assays, the HCK inhibitor (MedChemExpress, Cat. No.: HY15764) was used at 200 nM, and buparvaquone (MedChemExpress, Cat. No.: HY17581) at 100 nM for 72 or 96 h depending on the experiment.

2.2. Widefield immunofluorescence microscopy

Initially transfection of BoMacs were confirmed and monitored during selection for GFP expressing cells with a widefield immunofluorescence microscope (Leica DMI8). Upon establishment of stable GFP expressing cells, cells were grown on rounded coverslips and fixed with 4 % paraformaldehyde (Morphisto, Germany) for 10 min at room temperature. The cells were stained for Ta9 using polyclonal rat anti-Ta9 serum (1:500, diluted in PBS-1%BSA-0.4%Triton) for an hour at room temperature (RT). Secondary antibody was Alexa Fluor™ 594 goat anti-rat IgG (ThermoFisher, 1:500 dilution in PBS-0.4%Triton, 1 h at RT). To check HCK protein levels in Ta9-expressing BoMacs, an anti-HCK antibody (N30, Santa Cruz, sc-72) was used at a 1:250 dilution in the same dilution solution as described above. The secondary antibody used for detection was Alexa Fluor™ 594 goat anti-rabbit antibody

Table 1
List of bovine oncogenes or tumor suppressor genes whose expression were significantly altered in BoMac$^{GFP-Ta9}$.

Gene ID	Product name	Function	Direction of expression change (Fold change)	False discovery rate (FDR)
CDKN1A	Cyclin-dependent kinase inhibitor 1	Oncogene/ Tumor suppressor	Upregulated (+1.02)	1.21E-28
CCND1	Cyclin D1	Oncogene	Upregulated (+1.13)	2.76E-16
ETV4	ETS translocation variant 4	Oncogene	Upregulated (+1.65)	0.00375923
ETV5	ETS translocation variant 5	Oncogene	Upregulated (+2.01)	4.96E-10
FLI1	Friend leukemia integration 1	Oncogene	Upregulated (+3.79)	1.11E-101
FRA1	Fos-related antigen 1	Oncogene	Upregulated (+1.27)	1.57E-08
GLI2	Glioma-Associated Oncogene Family Zinc Finger 2	Oncogene	Upregulated (+1.17)	0.00038047
GRO1	Growth-Regulated Oncogene 1	Oncogene	Upregulated (+3.09)	3.87E-09
HCK	Hematopoietic Cell Kinase	Oncogene	Upregulated (+3.95)	1.49E-30
IL7R	Interleukin 7 Receptor	Oncogene	Upregulated (+1.57)	2.29E-10
MYB	Myeloblastosis	Oncogene	Downregulated (−1.17)	1.95E-07
MYBL1	Myb proto-oncogene like 1	Oncogene	Upregulated (+1.14)	6.58E-28
MYCN	N-myc proto-oncogene	Oncogene	Upregulated (+1.18)	0.0001711
RASGRP1	RAS guanyl-releasing protein 1	Tumor suppressor	Upregulated (+1.5)	2.31E-44
PIM1	Proto-oncogene serine/ threonine-protein kinase	Oncogene	Upregulated (+1.04)	7.97E-10
TAL1	T-cell acute lymphocytic leukemia protein 1	Oncogene	Upregulated (+3.9)	1.95E-08
WNT5B	Protein Wnt-5b	Oncogene/ Tumor suppressor	Upregulated (+1.17)	7.37E-09

(ThermoFisher) at a 1:500 dilution. The coverslips were then mounted on microscopic slides in medium containing DAPI dye (ROTI®Mount FluorCare, Carl Roth, Germany, Art. No. HP20.1) to visualize nuclei. Images of BoMacs stably expressing GFP and GFP-Ta9 were taken using Leica DMI8 microscope. Captured images were processed in Fiji Image J software.

2.3. Western blotting for GFP expression

Equal numbers of stable GFP and GFP-Ta9 expressing macrophages were lysed using a commercial cell lysis buffer (ChromoTek GFP-Trap™ kit, Proteintech) containing Halt™ protease inhibitor cocktail (Thermo Scientific, Cat. No. 87786) and PhosSTOP™ phosphatase inhibitors (Roche, Cat. No. 04906845001). Lysates were mixed with 4X Laemmli buffer (ROTI®Load, Carl Roth, Art. No. K929.2) and boiled for 5 min at 95 °C. Equal amounts of lysate were loaded into wells of 12 % Mini-PROTEAN® TGX 4–20 % pre-cast protein gels (BIO-RAD, #4561094) installed in Mini-PROTEAN® tetra vertical electrophoresis cell, filled with 1X TG-SDS solution (ROTIPHORESE®, Carl Roth, Germany, Art. No. 3060.3). The gels were run for 1 h at constant 150 V. Proteins were transferred to nitrocellulose membranes by electroblot and membranes blocked for 1 h at room temperature in PBS solution containing 5 % W/V skim milk (Sigma-Aldrich). The blots were then incubated with HRP-conjugated anti-GFP antibody (GeneTex, GTX113618-01, 1/10000 dilution in PBS-0.1 % TWEEN® 20 (Merck)- 1 % BSA solution, 1 h at room temperature), or mouse monoclonal anti-α-tubulin antibody (Sigma-Aldrich®, T5168; 1/4000 dilution in PBS-0.1 % TWEEN- 1 % BSA solution, overnight at 4 °C). Secondary antibody for α-tubulin (Chicken anti-mouse IgG conjugated with HRP, Santa Cruz, sc-2954) was diluted in the same PBST-BSA solution (1:5000) and incubated with the membrane for 1 h at room temperature. Protein bands were rendered visible by adding Pierce™ ECL western blotting substrate (Thermo Scientific, Cat. No. 32109) on the filters and images taken using a Fusion Western blot imaging machine (Vilber Lourmat).

2.4. RNA sequencing, identification of differentially expressed genes (DEGs) and KEGG and GO pathway enrichment analysis

Total RNA was extracted from three independent BoMac^{GFP} and BoMac$^{GFP-Ta9}$ cell lines. The quality and quantity of RNA was initially measured by a NanoDrop 1000 (Thermofisher), before processing by Agilent 2100 machine. Qualified RNA were then processed for library construction. The procedures are described as follows: mRNA was isolated by Oligo(dT)-attached magnetic beads and mRNA was then randomly fragmented in fragmentation buffer. First-strand cDNA was synthesized with fragmented mRNA as template and random hexamers as primers, followed by second-strand synthesis with addition of PCR buffer, dNTPs, RNase H and DNA polymerase I. Purification of cDNA was processed with AMPure XP beads. Double-strand cDNA was subjected to end repair. Adenosine was added to the ends and ligated to adapters. AMPure XP beads were then applied to select fragments within a size range of 300–400 bp. A cDNA library was obtained by rounds of PCR on cDNA fragments generated from the previous step. In order to ensure the quality of the library, Qubit 2.0 and Agilent 2100 were used to examine the concentration of cDNA and insert size. Q-PCR was processed to obtain a more accurate library concentration. A library with a concentration larger than 2 nM is considered acceptable. The qualified library was pooled based on a pre-designed target data volume and then sequenced on the Illumina NovaSeq 6000 sequencing platform (BMKGENE). Based on sequencing-by-synthesis (Sequencing By Synthesis, SBS) technology, cDNA libraries were sequenced on Illumina high-throughput platform, generating significant amounts of high-quality raw data, saved in FASTQ format. Raw data (raw reads) of FASTQ format were firstly processed through in-house perl scripts. In this step, clean data (clean reads) were obtained by removing reads containing adapter, reads containing ploy-N and low quality reads from raw data. At the same time, Q20, Q30, GC-content and sequence duplication level of the clean data were calculated. The Phred Quality Score (Q-Score) represents the probability of a base-calling error, calculated as $Q = -10 \times \log_{10}(P)$, where P is the error probability. Higher Q-scores indicate greater base-calling accuracy (e.g., Q20 = 99 %, Q30 = 99.9 %). All the downstream analyses were based on clean data with high quality. A total of 6 samples were processed for transcriptome sequencing, generating 44.42 Gb of clean data. At least 6.80 Gb clean data were generated for each sample with a minimum 94.51 % of clean data achieving a quality score of Q30. The clean data were further mapped to a pre-defined reference genome (Bos_taurus. GCF_002263795.2.genome.fa) generating mapped data. The HISAT2 [41] system, a more advanced version of TopHat2/Bowtie2, was used for mapping RNA-seq reads. HISAT2 uses a Burrows-Wheeler Transform and Ferragina-Manzini (FM) index based search. The mapping ratio of each sample against the reference genome ranged from 97.65 % to 98.02 %. StringTie [42] was applied to assemble the mapped reads. The algorithm is established based on optimality theory and utilizes a novel

Table 2
Bovine inflammation associated genes differentially expressed in BoMac$^{GFP-Ta9}$.

Gene ID	Product name	Category	Direction of expression change	False discovery rate (FDR)
IL6	Interleukin 6	Cytokine	Upregulated (+4.23)	3.98E-09
IL18	Interleukin 18	Cytokine	Upregulated (+1.29)	2.52E-31
GRO1 (CXCL1)	Growth-Regulated Oncogene 1	Chemokine (IL8- like)	Upregulated (+3.09)	2.50E-06
CXCL3	Chemokine (C-X-C motif) ligand 3	Chemokine	Upregulated (+1.72)	3.10E-10
CXCL5	C-X-C motif chemokine 5	Chemokine	Upregulated (+4.73)	1.61E-62
CXCL9	Chemokine (C-X-C motif) ligand 9	Chemokine	Upregulated (+1.83)	4.40E-36
CXCL11	C-X-C motif chemokine 11	Chemokine	Upregulated (+2.2)	2.50E-06
TGFB1	Transforming growth factor beta 1	Growth factor	Upregulated (+1.43)	1.33E-61
CTGF	Connective tissue growth factor	Growth factor	Upregulated (+1.35)	0.00021033
VGF	Nerve growth factor inducible	Growth factor	Upregulated (+1.76)	0.00268585
VEGFC	Vascular endothelial growth factor	Growth factor	Upregulated (+1.27)	1.15E-12
FGF1	Fibroblast growth factor	Growth factor	Upregulated (+2.09)	9.01E-40
CXCR4	C-X-C chemokine receptor type 4	Receptor	Upregulated (+1.84)	9.50E-09
IL7R	Interleukin 7 Receptor	Receptor	Upregulated (+1.57)	2.29E-10
TNFRSF1B	Tumor necrosis factor receptor superfamily member 1B	Receptor	Upregulated (+1.37)	1.84E-07
TNFRSF11B	Tumour necrosis factor receptor superfamily member 11B	Receptor	Upregulated (+1.93)	6.59E-15
IL20RA	Interleukin 20 Receptor Subunit Alpha	Receptor	Downregulated (−1.76)	1.67E-07
IL17RE	Interleukin 17 Receptor E	Receptor	Downregulated (−1.14)	0.0001542
MMP2	Matrix metalloproteinase 2	Metalloproteinase	Upregulated (+3.68)	3.06E-27
ADAMDEC1	ADAM-like, decysin 1	Metalloproteinase	Upregulated (+9.55)	1.09E-13
ADAMTS3	A disintegrin and metalloproteinase with thrombospondin motifs 3	Metalloproteinase	Upregulated (+1.62)	3.20E-56
ADAMTS16	A disintegrin and metalloproteinase with thrombospondin motifs 16	Metalloproteinase	Upregulated (+1.46)	3.81E-27
FN1	Fibronectin	Extracellular matrix (ECM)	Upregulated (+1.09)	1.74E-25
COL2A1	Collagen type III, alpha-1 chain	ECM	Upregulated (+1.36)	1.68E-07
COL3A1	Collagen type III, alpha-1 chain	ECM	Upregulated (+1.02)	1.27E-15
COL7A1	Collagen type VII, alpha-1 chain	ECM	Upregulated (+1.86)	4.24E-35
COL11A2	Collagen type XI, alpha-2 chain	ECM	Upregulated (+2.27)	4.01E-20

network flow algorithm, as well as an optional de novo assembly step, to assemble and quantify transcripts representing multiple spliced variants for each gene locus. The number of fragments from a transcript is affected by sequencing data volume (or number of mapped reads), length of the transcript, expression level of transcripts. In order to reveal the expression level of each transcript more accurately, the number of mapped reads was normalized by the length of its transcripts. FPKM (Fragments Per Kilobase of transcript per Million fragments mapped) was applied to measure the expression level of a gene or transcript by StringTie using maximum flow algorithm. The equation for FPKM is shown below:

$$\text{FPKM} = \frac{\text{cDNA Fragments}}{\text{Mapped Fragments (Millions) X Transcript Length (kb)}}$$

In the equation, cDNA Fragments represents the number of PE reads mapped to the specific transcript; Mapped Fragments (Millions) is the number of all mapped reads, which is counted as 10^6; Transcript Length (kb) is the length of transcript in unit of 10^3 b.

Differential expression analysis was processed by DESeq2 [43]. The criteria for differentially expressed genes was set as Fold Change (FC)≥1 and FDR<0.01. Fold change (FC) refers to the ratio of gene expression between two samples. False Discovery Rate (FDR) refers to an adjusted p-value used to measure the significance of the gene expression difference. Hierarchical clustering analysis was processed on differentially expressed genes, i.e. genes with the same or similar expression profiles were clustered together. Principal component analysis (PCA) was performed using FPKM data for each sample. Similarity among samples was displayed by reducing dimensionality into two or three principal components.

KEGG [44] is a database resource for understanding high-level functions and utilities of the biological system, such as the cell, the organism and the ecosystem, from molecular-level information, especially large-scale molecular datasets generated by genome sequencing and other high-throughput experimental technologies (http://www.genome.jp/kegg/). We used KOBAS [45] software to test the statistical enrichment of differential expression genes in KEGG pathways. The KEGG annotations of DEGs were classified according to the type of pathways.

To test if KEGG pathways are over-presented within the Ta9 DEG data set, enrichment factors and fisher test were applied for determination of enrichment degree and significance. Gene Ontology (GO) enrichment analysis of the differentially expressed genes (DEGs) was implemented by the GOseq R packages based on Wallenius non-central hyper-geometric distribution [46] which can adjust for gene length bias in DEGs.

2.5. mRNA expression analysis by quantitative real time qRT-PCR (qRT-PCR)

Total RNA was extracted from BoMac^{GFP} and BoMac$^{GFP-Ta9}$ by using NucleoSpin RNA plus (Macherey Nagel, REF: 740984.50). Five-hundred nanograms of RNA was converted to cDNA by the Protoscript II first strand cDNA synthesis kit (New England Biolabs, Cat. No. E6560S). cDNA from each sample was diluted 1:20 in DNase free water. The PCR reaction (20 μl) included 0.5 μl of each forward and reverse primers at 10 μM, 10 μl SYBR green mix (Luna® Universal qPCR Master Mix, New England Biolabs, Cat. No. M300S), 2 μl diluted cDNA and 7 μl molecular grade water. Bovine HCK primers were forward: ATCCCTGGTGTGCAAGATCG; reverse: ACTTGATGGGGAACTTGGCC. mRNA levels were normalized to bovine GAPDH with forward: GTTCAACGGCACAGTCAA and reverse: TCACGCCCATCACAAAC primers [47]. $2^{-\Delta\Delta CT}$ Method was used to calculate relative mRNA expression levels [48].

2.6. Cell proliferation assay

Theileria-transformed cells were seeded in 24 well cell culture plates (of 1–2 X 10^5 cells/ml) with or without the drugs. To obtain proliferation curves, the cells were manually counted using a Neubauer hemocytometer every 24 h for a duration of 3–4 days. The percentage inhibition of cell proliferation was estimated by dividing the number of cells counted in treatment groups divided by the number of cells counted from the drug free control group at the final counting time point.

2.7. Culturing Theileria transformed leukocyte cells in soft agar

Cells were initially cultured in absence or presence of drugs for 72 h,

Table 3
Transcription factor enrichment in differentially expressed bovine genes in response to *Theileria annulata* Ta9.

Rank	Transcription factor	FET p-value	False discovery rate (FDR)	Odds Ratio
1	MTF2	3,82E-18	1,17E-15	2512
2	TP53[a]	1,46E-09	2,23E-07	2,66
3	TCF3	2,03E-08	1,87E-06	2078
4	SMAD4[a]	2,70E-08	1,87E-06	1984
5	SMAD3[a]	3,04E-08	1,87E-06	2378
6	POU5F1	7,54E-08	3,86E-06	2052
7	ZNF217	1,26E-07	5,50E-06	2153
8	FOXA2	1,57E-07	6,00E-06	1805
9	AR	2,10E-07	7,17E-06	1738
10	WT1	4,63E-07	1,31E-05	1736
11	ESR1	4,70E-07	1,31E-05	2129
12	BACH1	5,65E-07	1,44E-05	2,13
13	PRDM14	7,91E-07	1,87E-05	1981
14	RUNX2	1,41E-06	3,09E-05	1698
15	NR3C1	4,40E-06	7,95E-05	2334
16	TCF21	5,09E-06	8,69E-05	1843
17	OLIG2	6,88E-06	1,11E-04	1856
18	KLF4	8,81E-06	1,35E-04	1,98
19	NANOG	9,26E-06	1,35E-04	1,88
20	CEBPD	1,72E-05	2,40E-04	2707
21	SOX2	2,67E-05	3,41E-04	1588
22	STAT3[a]	2,91E-05	3,58E-04	1606
23	SRY	3,51E-05	4,14E-04	1615
24	ARNT	3,64E-05	4,14E-04	2071
25	PPARD	4,95E-05	5,43E-04	3821
26	TCF4	5,62E-05	5,75E-04	1531
27	RELA[a]	7,18E-05	7,11E-04	1912
28	REST	8,72E-05	8,36E-04	1691
29	ZIC3	1,25E-04	0,00113	2919
30	MNX1	1,43E-04	0,00122	1719
31	JUN[a]	1,43E-04	0,00122	1768
32	NFE2L2	3,36E-04	0,00229	1898
33	GABPA	3,36E-04	0,00229	1898
34	NR0B1	4,24E-04	0,00277	1718
35	SALL4	5,48E-04	0,00339	1954
36	GBX2	6,05E-04	0,00364	2944
37	SOX9	7,55E-04	0,00437	1613
38	TP63	8,01E-04	0,00456	1439
39	STAT6	0,001297	0,00675	2,3
40	TBX3	0,001345	0,00688	1827
41	AHR	0,001788	0,00871	1936

[a] relevant to *Theileria*-induced leukocyte transformation.

washed once with PBS and counted. A two-layer low melting temperature agarose (Carl Roth, Germany, Art. No. 6351.1) was prepared by a 1:1 dilution with 2X complete DMEM F12 medium (Sigma-Aldrich, D9785) containing 20 % FBS and 200 U/ml Penicillin/Streptomycin. First, the base acellular layer (1.5 ml of 1 % percent agarose) was laid in each well of a six-well culture plate (Sarstedt, Germany). Following solidification of the base layer, the second cellular layer (1.5 ml of 0.7 % agarose) including 10,000 cells per well was added. The cell-containing layer was covered with 2 ml complete RPMI1640 medium that was refreshed twice per week. Colonies were fixed and stained with 0.0001 % crystal violet solution in methanol at 21 days post cell seeding until all colonies were stained blue. Next, the wells were rigorously washed with distilled water until the background pale blue color of the agarose gel turned colorless. This allowed imaging of the plates with the camera of an iPhone 12 on a white background. The images were then transferred to Fiji image J software for further processing.

2.8. Statistical analysis

Data were analyzed using two-tailed Student's *t*-tests. Results are expressed as the mean ± standard deviation. In the figures, statistical significance is denoted by $p < 0.05$ (*).

3. Results

3.1. Generation of bovine macrophages stably expressing GFP-tagged Ta9

We have shown that exogenous expression of Ta9 activates AP-1-driven transcription [35] and significantly, the *T. parva* genome encodes an orthologue of Ta9 (Tp9) [31], whilst the non-transforming *T. orientalis* does not. Similar to *T. annulata*-transformed leukocytes, *T. parva*-transformed B and T cells also display constitutive activation of AP-1 [9]. One important transcriptional target of AP-1 is matrix metalloproteinase 9 (*mmp9*), a major driver of *Theileria*-transformed leukocyte dissemination [49–51]. Secretion of Ta9/Tp9 and activation of AP-1 therefore appear to be a common major effector of parasite virulence [52]. For these reasons, we asked to what extent does the unique expression of Ta9 impact on macrophage transcription over and above activation of AP-1. To this end, we transfected GFP-tagged Ta9 into a bovine macrophage cell line (BoMac$^{GFP-Ta9}$), selected a stable cell line and performed RNA-Seq relative to a GFP alone transfected control line. The expression levels were lower when GFP was fused to Ta9 compared to GFP alone (Fig. 1A and B). GFP distribution confirmed cytoplasmic localization of Ta9 in BoMac$^{GFP-Ta9}$, as recently described for *T. annulata*-transformed macrophages [36].

3.2. Ta9 expression in bovine macrophages results in deregulated expression of multiple genes involved in oncogenesis and inflammation

To obtain a global view of bovine macrophage genes whose transcription is potentially affected by expression of Ta9, we performed RNA-sequencing for BoMac^{GFP} and BoMac$^{GFP-Ta9}$ cell lines. Principal component analysis (PCA) showed good clustering and separation of the samples representing each line (Fig. 2A). A hierarchical clustering heat map of all DEGs highlighted that the gene expression differences between the two lines showed a strong degree of consistency across replicate samples (Fig. 2B). Four hundred genes were expressed significantly higher (log2FC $\geq$ 1; FDR $<$0.01) and 160 genes were expressed at lower level in the TA9 expressing line (Fig. 2C) (Supplementary Table 1). Based on the Kyoto Encyclopedia of Genes and Genomes (KEGG) pathway classification, the highest number of DEGs were categorized in cancer associated pathways, but DEGs were also significantly enriched in cytokine and chemokine receptor signalling (Fig. 2D). The KEGG classification identified Ta9-DEGs as oncogenes, tumor suppressors and inflammation-associated genes. Strikingly, many oncogenes (*CCND1*, *CKDN1A, ETV4*, *ETV5*, *FLI1*, *FRA1*, *GLI2*, *GRO1*, *HCK*, *IL7R*, *MYBL1*, *MYCN*, *PIM1* and *TAL1*) were identified in the Ta9-elevated group (Table 1). Both microarray and RNA-Seq analyses previously identified expression of HCK and PIM1 to be infection-induced in *T. annulata*-transformed B cells (TBL20) compared to their non-infected counterparts (BL20) [19,20].

Expression of multiple inflammation-associated genes increased under the influence of Ta9. These included cytokines (*IL6* and *IL18*), chemokines (*CXCL1*, *CXCL3*, *CXCL5*, *CXCL9* and *CXCL11*), growth factors (*TGFB1*, *CTGF*, *VGF*, *VEGFC* and *FGF1*), cell surface receptors (*CXCR4*, *IL7R*, *TNFRSF1B* and *TNFRSF11B*), secreted effector molecules (*MMP2*, *ADAMDEC1*, *ADAMTS3* and *ADAMTS16*) and components of the extracellular matrix (*FN*, *COL2A1, COL3A1*, *COL7A1* and *COL11A2*) (Table 2). Consistent with this, gene ontology (GO) analysis performed on the 'Cellular Component' of Ta9-DEGs revealed an enrichment of genes coding for proteins of the extracellular space and extracellular matrix (Supplementary Fig. 1).

Ta9-DEGs were investigated to identify specific transcription factor (s) that might indicate which macrophage signaling pathways are impacted by Ta9 expression. Transcription factor enrichment analysis was performed using the publicly available online tool Chip-X Enrichment Analysis (ChEA3) and exploited the ChEA 'literature' library that mines published data (https://maayanlab.cloud/chea3/) [53]. A significant (0.01>FDR) enrichment of 40 bovine transcription factors was

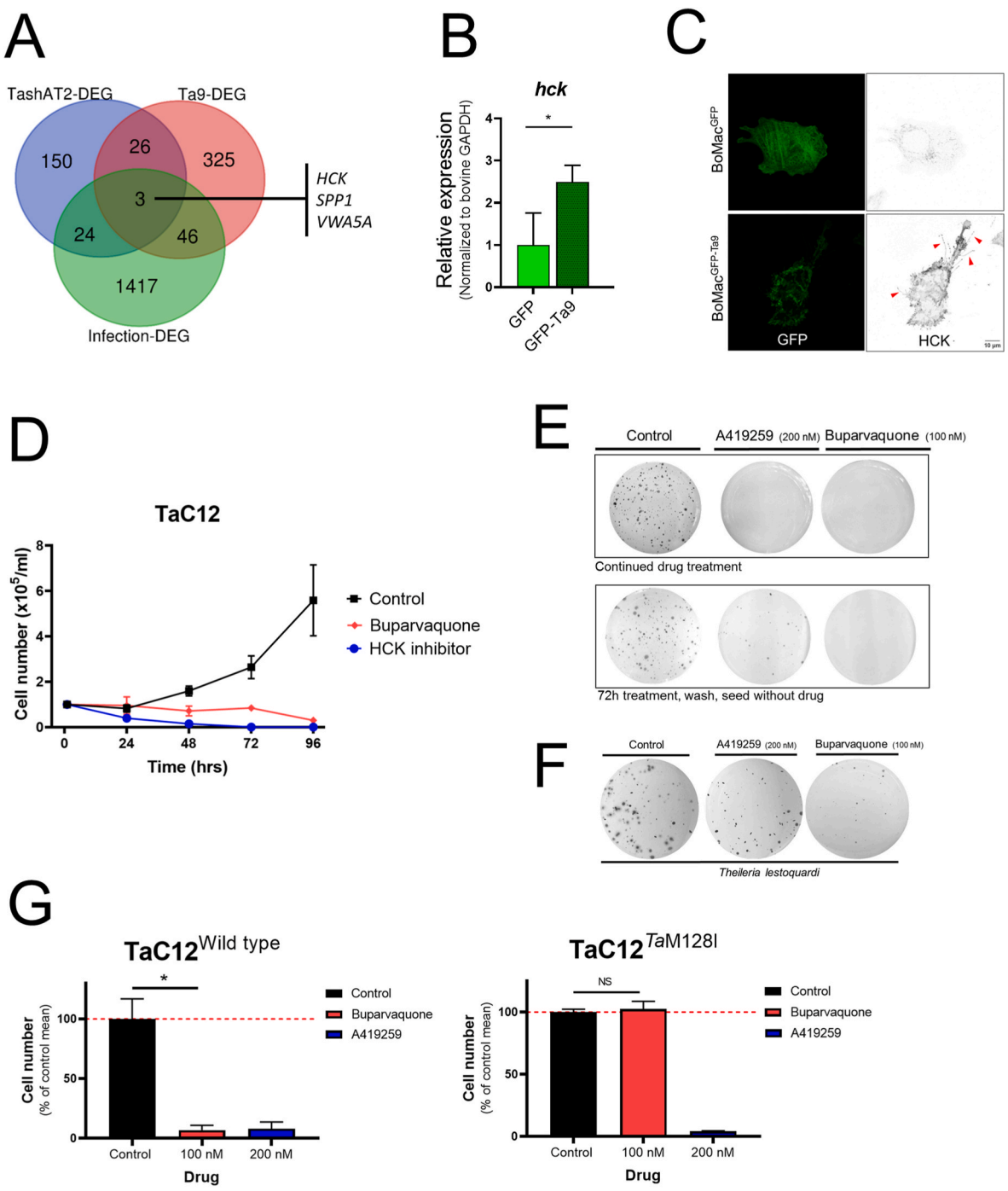

Fig. 3. The tyrosine kinase HCK is important for *Theileria*-induced leukocyte transformation. **A**, Merging RNA-seq datasets identified *HCK*, *VWA5A* and *SPP1* as putative co-modulated, infection-associated genes. Venn diagram was created with (https://bioinformatics.psb.ugent.be/webtools/Venn/). **B**, Confirmation of upregulated *hck* expression by qRT-PCR in bovine macrophages stably expressing GFP-tagged Ta9 compared to control GFP-only macrophages. mRNA expression levels were normalized to bovine *GAPDH* that did not show a significant change between samples in the RNA-seq analyses. Two-tailed student's t-test used to estimate significance. Mean fold change in mRNA expression level ± standard deviations shown. Results are representative of two independent experiments. *, p value < 0.05. **C**, Confirmation of increased HCK protein levels in Ta9-expressing BoMacs by immunofluorescence staining. Notably, in the presence of Ta9, macrophages developed membrane protrusions and microspikes (red arrowheads), which serve as indirect indicators of increased HCK activity. **D**, The HCK inhibitor A419259 (200 nM) blocks proliferation of *T. annulata*-transformed macrophages. Buparvaquone (100 nM) was used as a positive control. **E**, Two different treatment regimens were undertaken to evaluate efficacy of A419259 on *Theileria*-mediated macrophage transformation estimated in a soft agar colony formation assay. The first regimen included continued treatment of cells prior to seeding and during culture in soft agar with either the HCK inhibitor or buparvaquone. In the second regimen, cells were treated once for 72 h prior to seeding in agar and then cultured in agar for 21 days in absence of drugs, lower panel of images. **F**, A 'one-time' treatment strategy was applied to *T. lestoquardi*-transformed sheep leukocytes. Soft agar experiments were repeated at least two times each with three technical replicates. **G**, The HCK inhibitor blocks proliferation of both *T. annulata*-transformed macrophages harboring wild type parasites, or buparvaquone-resistant parasites. The Bar graph shows the impact of 96-h drug exposure on transformed cell numbers expressed as % inhibition compared with controls. Two-tailed student's t-test used to estimate significance. Results are representative of two independent experiments. *, p value < 0.05. NS, not significant.

found in the list of Ta9-DEGs (Table 3). Although not ranked among the top transcription factors, as expected [35] the AP-1 member c-JUN was enriched. The list also contained several other interesting and *Theileria* infection-relevant transcription factors such an NF-κB member v-rel avian reticuloendotheliosis viral oncogene homolog A (RELA), also known as p65 [26], Mothers Against Decapentaplegic homolog 3 & 4 (SMAD3 & SMAD4, TGF-β signaling) [54], Signal Transducer and Activator of Transcription 3 (STAT3) [15] and TP53 [55,56]. The highest scored transcription factor was MTF2 (Metal Response Element Binding Transcription Factor 2) which is a member of Polycomb repressive complex and possess both oncogenic and tumor suppressor roles in different cellular contexts [57]. Taken together, the RNA-Seq profiling of bovine macrophages expressing a single *T. annulata* gene (TA15705) coding for the protein Ta9 predicted upregulation of multiple host cell transcription factors associated with driving transcription of genes participating in inflammatory and oncogenic processes.

3.3. Ta9 upregulates expression of host proto-oncogene HCK, whose activity is essential for proliferation of Theileria-transformed leukocytes

A recent RNA-Seq study explored the contribution of *T. annulata* TashAT2 that is secreted and trafficked to the host nucleus to modulate expression of bovine genes in the same macrophage cell line BoMac [58]. Since Both Ta9 and TashAT2 are consistently found in the cytoplasm and nucleus of *T. annulata*-transformed bovine leukocytes, respectively, we wondered to what extent the transcription modulating activity of Ta9 and TashAT2 converge to generate perhaps a synergistic effect on host cell gene expression in infected leukocytes. To this end, we merged the list of Ta9 modulated genes identified (*i.e.* 560 genes) with those of TashAT2 (*i.e.* 206 genes with log2FC > 1; q value < 0.01) and also the full list of infection associated genes previously established by comparing *T. annulata*-infected B lymphocytes (TBL20) to non-infected B lymphocytes (BL20) [20]. Three DEG genes were over-represented across the three datasets (Fig. 3A): hematopoietic cell kinase (*HCK*), Von Willebrand Factor A Domain Containing 5A (*VW5A*) and Secreted Phosphoprotein 1, also known as Osteopontin (*SPP1*). We focused on HCK as it is known to be involved in cancer [28,59] and has previously described as being upregulated in *T. parva*-transformed B cells and *T. annulata*-transformed macrophages [22,29]. We first confirmed that the expression of hck was greater in BoMac$^{GFP-Ta9}$ compared to BoMac^{GFP} by qRT-PCR (Fig. 3B) and further validated the increased HCK protein levels using immunofluorescence imaging (Fig. 3C). Treatment at the nanomolar range of *T. annulata*-transformed macrophages (TaC12 cell line) with the potent HCK inhibitor A419259 (also known as RK20449) [59,60] blocked proliferation, as measured by cell counting (Fig. 3D). Continuous HCK inhibitor treatment resulted in complete blockade of colony formation of macrophages, similar to buparvaquone. Single HCK inhibitor treatment prior to seeding in agar resulted in reduction of colonies in both A419259- and buparvaquone-treated groups; however, to a lesser extent compared to continuous exposure to drug. In addition, A419259 appeared less potent compared to buparvaquone in this 'one-time' treatment strategy (Fig. 3E). The drug inhibitory activity of A419259 was confirmed in another independent *T. annulata*-transformed leukocyte isolate (Ankara, Turkey) (Supplementary Fig. 2) and a *T. lestoquardi*-transformed leukocyte cell line from the Sudanese Atbara isolate (Fig. 3F). Since A419259 showed therapeutic potential *in vitro*, we tested if it could also block proliferation of *T. annulata*-transformed macrophages harboring buparvaquone-resistant parasites [40]. While buparvaquone could inhibit proliferation of transformed macrophages harboring wild type parasites, but not macrophages with buparvaquone resistant parasites, the HCK inhibitor was equally effective against both cell groups (Fig. 3G).

4. Discussion

Theileria annulata-transformed leukocytes display extensive modulation of their host gene expression profiles [19–21,58,61,62]. The intracellular presence of live *Theileria* parasites contributes to at least half of the altered expression levels observed in transformed leukocyte gene expression, as upon elimination of the parasite by buparvaquone approximately half of the infection-induced deregulated genes revert to pre-infection expression levels [19]. Candidate effectors are *Theileria* secreted proteins that are trafficked to the host nucleus. A family of 17 parasite genes named the Tash family code for secreted proteins that possess nuclear localization signals and at least five proteins (TashAT1, TashAT2, TashAT3, SuAT1 and TashHN) have been identified in transformed cell nuclei and are not thought to be encoded by non-transforming *Theileria* species [54,63–66]. A recent study described another family of secreted proteins (nuclear intrinsically disordered proteins, NIDPs 1–4) in the transformed macrophage nucleus [36]. Herein, we have focused on another secreted protein Ta9 (TA15705) unique to transforming *Theileria* spp., since it has previously been shown to sustain AP-1-driven transcription [35]. Herein, we sought to understand to what level Ta9, as a demonstrated AP-1 activator, contributes to transcriptional changes of an infection-relevant host cell, the bovine macrophage.

RNA-seq mediated transcriptional profiling of BoMacs expressing a GFP-Ta9 fusion protein identified differential expression of genes involved in cancer-related pathways. The most striking finding was the upregulation of at least 17 oncogenes (Table 1) and more than 20 genes directly associated with inflammation (Table 2). Some of the identified oncogenes and inflammation related genes are highly relevant to tropical theileriosis and hematopoietic malignancies. Therefore, we performed an enrichment analysis on Ta9-elevated DEGs and this showed that Ta9 might be involved in activation of several transcription factors in addition to AP-1 (JUN), such as NF-κB (RELA) and STAT3 among others. It is difficult to precisely say how Ta9 activates AP-1 and the other transcription factors enriched in the list of Ta9-DEGs. One possible mechanism could be via Ta9-induced upregulation of tumor necrosis factor receptor B1 (*TNFRS1B*). TNF-α facilitates activation of both AP-1 and NF-κB signaling in *Theileria*-transformed macrophages and overexpression of a dominant negative version of TNFSRB2 downregulated NF-κB transcriptional activity in *T. parva* transformed cells [67,68]. Another potential mechanism could be through Ta9-mediated overexpression of AP-1 and NF-κB family members, a strategy that is employed by latent membrane protein (LMP-1) oncoprotein of Epstein-Barr virus to activate AP-1 and NF-κB pathways [69]. Interestingly, the Ta9-DEG list included Fos-related antigen 1 (*FRA1* or *FOSL1*; 1.2 +FC); a highly expressed infection induced gene, whose expression reverses upon parasite killing [19]. In addition, many Ta9-induced (associated) DEGs were significantly enriched for chemokine and cytokine receptor signaling, which could underpin augmented signaling of multiple host cell transcription factors. Examples include the pro-inflammatory cytokines IL6 and IL18, and the pro-oncogenic IL7 receptor (IL7R) [70,71].

We focused further on the contribution of Ta9-upregulated host cell proto-oncogene *hck*, because comparative transcriptome analysis of the Ta9-regulated gene dataset with that of infection deregulated genes, plus genes whose modulated expression was associated with overexpression of TashAT2 in BoMac highlighted *hck*, a gene whose expression is known to be induced upon infection [19–21]. Interestingly, *hck* was found to be strongly upregulated by Ta9 expression (significant +4.4-fold increase in RNA-seq reads and confirmed by qRT-PCR), upon infection (TBL20 vs BL20) [20], and also identified as displaying lower expression in TashAT2 transfected cells (significant −1.3-fold decrease in RNA-seq reads) [58]. The latter is an interesting observation, because high expression of *hck* is normally toxic for macrophages [72] and thus, it could be that in *T. annulata*-transformed macrophages Ta9 induces *hck* and TashAT2 moderates the degree of induction to prevent cytotoxicity.

This would be in agreement with the previous observation that predicted a suppressive role in cancer associated traits of BoMacs expressing TashAT2 [58]. This leads to the notion that in the context of *Theileria*-induced leukocyte transformation, TashAT2 may create a balance in expression of genes, whose over induction by other parasite factors (*e.g.* Ta9) could be detrimental to the survival of the infected leukocyte. Similar results have previously been found, notably for Interferon-stimulated gene 15 (ISG15). ISG15 is induced in infected B cells (TBL) vs non-infected B cells (BL), reduced by TashAT2 and elevated by buparvaquone treatment [73]. Indeed, quite a number of genes show this type of modulated profile in infected cells [19].

It is noteworthy that the human *hck* promoter possess binding sites for AP-1 [74], and we also detected (not shown) consensus AP-1 binding sites in the promoter of bovine *hck* (PROMO v3.0 program, https://alggen.lsi.upc.es/cgi-bin/promo_v3/promo/promoinit.cgi?dirDB=TF_8.3). In *T. parva*-transformed B cells HCK is constitutively active and contributes to heightened AP-1 activity. The constitutive activation of HCK was ascribed to infection-induced exclusion of the negative regulator C-terminal Src kinase (CSK) from lipid rafts, where location of HCK was demonstrated [22]. One could hypothesize that a secreted parasite protein is involved in sequestering CSK, or directly binds and activates HCK. Thus, it seems that *T. annulata* uses several factors to affect HCK activity, TashAT2 and Ta9 to modulate host *hck* expression and another unidentified factor to sequester CSK. Similarly, Ta9 and a secreted parasite prolyl isomerase, TaPIN1, potentiate AP-1 signaling. This targeting of a specific host locus by multiple parasite factors seems to be a common apicomplexan strategy, as a recent genome-wide loss-of-function screen identified four *Toxoplasma gondii* genes (TgIST, GRA16, GRA24, and GRA28) required for a complete block of the IFN-γ response [75]. In addition, targeting expression of a host gene by a combination of parasite effectors could be a strategy to ensure parasite survival in different cellular contexts such as leukocytes (B cell, T cell and macrophage for *Theileria*) and for all nucleated cells for *Toxoplasma*.

Ta9-expression induced heightened HCK levels and A419259 inhibition of HCK enzymatic activity demonstrated it is essential for proliferation of *Theileria*-transformed leukocytes. Several past studies have shown that proliferation of *Theileria*-transformed leukocytes is susceptible to general Src kinase inhibitors [22,23,26], and a recent drug screen reported high inhibitory activity of Dasatinib (an inhibitor of the Src kinase, BCR-ABL kinase and other tyrosine kinases) against *T. parva*-transformed cells [76]. We confirmed Dasatinib treatment also blocks proliferation of *T. annulata* transformed macrophages (not shown). Since Dasatinib and A459259 target host Src kinases they have the potential to be efficacious to counter the spread of parasite resistance to buparvaquone [77–79], the drug primarily in current use to treat tropical theileriosis. Further work is required to demonstrate a suitable therapeutic index for clinical application. Nevertheless, herein we have shown *in vitro* that a combination of upregulated *hck* expression and increased HCK enzymatic activity are essential for *Theileria* to exploit fully its leukocyte transforming ability and provide, therefore, a target mechanism for therapeutic intervention. Future work will aim to identify the host leukocyte proteins interacting with Ta9 in the cytosol and nucleus and elucidation of TA9-dependent AP1 activation.

5. Conclusions

Large-scale transcriptome data highlighted secreted Ta9 is a candidate as an important *T. annulata* virulence factor in the pathogenesis of tropical theileriosis via activation of AP1 and modulation of host cell gene expression. We also propose that Ta9 may act in concert with other secreted *Theileria* factors to fine tune the bovine transcriptome, as both Ta9 and TashAT2 were found to be linked to altered *hck* expression.

CRediT authorship contribution statement

Shahin Tajeri: Writing – review & editing, Writing – original draft, Visualization, Validation, Software, Resources, Methodology, Investigation, Formal analysis, Data curation, Conceptualization. **Brian Shiels:** Writing – review & editing, Supervision, Resources, Conceptualization. **Gordon Langsley:** Writing – review & editing, Writing – original draft, Supervision, Resources, Conceptualization. **Ard Menzo Nijhof:** Writing – review & editing, Writing – original draft, Supervision, Resources, Project administration, Funding acquisition, Conceptualization.

Data availability

Raw RNA-Seq reads have been uploaded to the European Nucleotide Archive (https://www.ebi.ac.uk/ena/) under the study accession number PRJEB77601.

Declaration of competing interest

The authors declare the following financial interests/personal relationships which may be considered as potential competing interests: Shahin Tajeri reports article publishing charges was provided by Free University of Berlin. Shahin Tajeri reports a relationship with Free University of Berlin that includes: employment. If there are other authors, they declare that they have no known competing financial interests or personal relationships that could have appeared to influence the work reported in this paper.

Appendix A. Supplementary data

Supplementary data to this article can be found online at https://doi.org/10.1016/j.micpath.2024.107252.

References

[1] C.G.D. Brown, D.A. Stagg, R.E. Purnell, G.K. Kanhai, R.C. Payne, Infection and transformation of bovine lymphoid cells in vitro by infective particles of *Theileria parva*, Nature 245 (1973) 101–103.
[2] C. von Schubert, G. Xue, J. Schmuckli-Maurer, K.L. Woods, E.A. Nigg, D.A. E. Dobbelaere, The transforming parasite *Theileria* co-opts host cell mitotic and central spindles to persist in continuously dividing cells, PLoS Biol. 8 (2010) e1000499.
[3] W.I. Morrison, The aetiology, pathogenesis and control of theileriosis in domestic animals, Rev Sci Tech 34 (2015) 599–611.
[4] R. Bishop, A. Musoke, S. Morzaria, M. Gardner, V. Nene, *Theileria*: intracellular protozoan parasites of wild and domestic ruminants transmitted by ixodid ticks, Parasitology 129 (Suppl) (2004) S271–S283.
[5] S. Tajeri, M. Haidar, T. Sakura, G. Langsley, Interaction between transforming *Theileria* parasites and their host bovine leukocytes, Mol. Microbiol. 115 (2021) 860–869.
[6] K. Cheeseman, J.B. Weitzman, Host–parasite interactions: an intimate epigenetic relationship, Cell Microbiol. 17 (2015) 1121–1132.
[7] K. Tretina, H.T. Gotia, D.J. Mann, J.C. Silva, *Theileria*-transformed bovine leukocytes have cancer hallmarks, Trends Parasitol. 31 (2015) 306–314.
[8] D. Dobbelaere, V. Heussler, Transformation of leukocytes by *Theileria parva* and *T. annulata*, Annu. Rev. Microbiol. 53 (1999) 1–42.
[9] C. Botteron, D. Dobbelaere, AP-1 and ATF-2 are constitutively activated via the JNK pathway in *Theileria parva*-transformed T cells, Biochem. Biophys. Res. Commun. 246 (1998) 418–421.
[10] M. Chaussepied, D. Lallemand, M.-F. Moreau, R. Adamson, R. Hall, G. Langsley, Upregulation of Jun and Fos family members and permanent JNK activity lead to constitutive AP-1 activation in *Theileria*-transformed leukocytes, Mol. Biochem. Parasitol. 94 (1998) 215–226.
[11] J. Schmuckli-Maurer, J. Kinnaird, S. Pillai, P. Hermann, S. McKellar, W. Weir, et al., Modulation of NF-κB activation in *Theileria annulata*-infected cloned cell lines is associated with detection of parasite-dependent IKK signalosomes and disruption of the actin cytoskeleton, Cell Microbiol. 12 (2010) 158–173.
[12] V. Ivanov, B. Stein, I. Baumann, D.A. Dobbelaere, P. Herrlich, R.O. Williams, Infection with the intracellular protozoan parasite *Theileria parva* induces constitutively high levels of NF-kappa B in bovine T lymphocytes, Mol. Cell Biol. 9 (1989) 4677–4686.
[13] M. Metheni, N. Echebli, M. Chaussepied, C. Ransy, C. Chéreau, K. Jensen, et al., The level of H2O2 type oxidative stress regulates virulence of *Theileria*-transformed leukocytes, Cell Microbiol. 16 (2014) 269–279.
[14] S. Medjkane, M. Perichon, J. Marsolier, J. Dairou, J.B. Weitzman, *Theileria* induces oxidative stress and HIF1α activation that are essential for host leukocyte transformation, Oncogene 33 (2014) 1809–1817.

[15] F. Dessauge, S. Hilaly, M. Baumgartner, B. Blumen, D. Werling, G. Langsley, c-Myc activation by *Theileria* parasites promotes survival of infected B-lymphocytes, Oncogene 24 (2005) 1075–1083.

[16] M. Haidar, Z. Rchiad, H.R. Ansari, F. Ben-Rached, S. Tajeri, P. Latre De Late, et al., miR-126-5p by direct targeting of JNK-interacting protein-2 (JIP-2) plays a key role in *Theileria*-infected macrophage virulence, PLoS Pathog. 14 (2018) e1006942.

[17] M. Haidar, S. Tajeri, L. Momeux, T. Mourier, F. Ben-Rached, S. Mfarrej, et al., miR-34c-3p regulates protein kinase A activity independent of cAMP by dicing prkar2b transcripts in *Theileria annulata*-infected leukocytes, mSphere 8 (2023) e00526.

[18] J. Marsolier, S. Pineau, S. Medjkane, M. Perichon, Q. Yin, E. Flemington, et al., OncomiR addiction Is generated by a miR-155 feedback loop in *Theileria*-transformed leukocytes, PLoS Pathog. 9 (2013) e1003222.

[19] J.H. Kinnaird, W. Weir, Z. Durrani, S.S. Pillai, M. Baird, B.R. Shiels, A bovine lymphosarcoma cell line infected with *Theileria annulata* exhibits an irreversible reconfiguration of host cell gene expression, PLoS One 8 (2013) e66833.

[20] Z. Rchiad, M. Haidar, H.R. Ansari, S. Tajeri, S. Mfarrej, F. Ben Rached, et al., Novel tumour suppressor roles for GZMA and RASGRP1 in *Theileria annulata*-transformed macrophages and human B lymphoma cells, Cell Microbiol. 22 (2020) e13255.

[21] Z. Durrani, W. Weir, S. Pillai, J. Kinnaird, B. Shiels, Modulation of activation-associated host cell gene expression by the apicomplexan parasite *Theileria annulata*, Cell Microbiol. 14 (2012) 1434–1454.

[22] M. Baumgartner, P. Angelisová, N. Setterblad, N. Mooney, D. Werling, Vc Horejsi, et al., Constitutive exclusion of Csk from Hck-positive membrane microdomains permits Src kinase-dependent proliferation of *Theileria*-transformed B lymphocytes, Blood 101 (2003) 1874–1881.

[23] C. Fich, U. Klauenberg, B. Fleischer, B.M. BrÖKer, Modulation of enzymatic activity of Src-family kinases in bovine T cells transformed by *Theileria parva*, Parasitology 117 (1998) 107–115.

[24] Y. Galley, G. Hagens, I. Glaser, W. Davis, M. Eichhorn, D. Dobbelaere, Jun NH2-terminal kinase is constitutively activated in T cells transformed by the intracellular parasite *Theileria parva*, Proc. Natl. Acad. Sci. U.S.A. 94 (1997) 5119–5124.

[25] P. Latré De Laté, M. Haidar, H. Ansari, S. Tajeri, E. Szarka, A. Alexa, et al., *Theileria* highjacks JNK2 into a complex with the macroschizont GPI (GlycosylPhosphatidylInositol)-anchored surface protein p104, Cell Microbiol. 21 (2019) e12973.

[26] V.T. Heussler, S. Rottenberg, R. Schwab, P. Küenzi, P.C. Fernandez, S. McKellar, et al., Hijacking of host cell IKK signalosomes by the transforming parasite *Theileria*, Science. 298 (2002) 1033–1036.

[27] P. Hermann, D.A. Dobbelaere, *Theileria*-induced constitutive IKK activation is independent of functional Hsp90, FEBS Lett. 580 (2006) 5023–5028.

[28] A.R. Poh, R.J.J. O'Donoghue, M. Ernst, Hematopoietic cell kinase (HCK) as a therapeutic target in immune and cancer cells, Oncotarget 6 (2015).

[29] M. Baumgartner, *Theileria annulata* promotes Src kinase-dependent host cell polarization by manipulating actin dynamics in podosomes and lamellipodia, Cell Microbiol. 13 (2011) 538–553.

[30] M. Ma, M. Baumgartner, Filopodia and membrane blebs drive efficient matrix invasion of macrophages transformed by the intracellular parasite *Theileria annulata*, PLoS One 8 (2013) e75577.

[31] A. Pain, H. Renauld, M. Berriman, L. Murphy, C.A. Yeats, W. Weir, et al., Genome of the host-cell transforming parasite *Theileria annulata* compared with *T. parva*, Science. 309 (2005) 131–133.

[32] W. Weir, J. Sunter, M. Chaussepied, R. Skilton, A. Tait, E.P. de Villiers, et al., Highly syntenic and yet divergent: a tale of two Theilerias, Infect. Genet. Evol. 9 (2009) 453–461.

[33] S. Tajeri, G. Langsley, *Theileria* secretes proteins to subvert its host leukocyte, Biol. Cell. 113 (2021) 220–233.

[34] N.D. MacHugh, W. Weir, A. Burrells, R. Lizundia, S.P. Graham, E.L. Taracha, et al., Extensive polymorphism and evidence of immune selection in a highly dominant antigen recognized by bovine CD8 T cells specific for *Theileria annulata*, Infect. Immun. 79 (2011) 2059–2069.

[35] A.H. Unlu, S. Tajeri, H.B. Bilgic, H. Eren, T. Karagenc, G. Langsley, The secreted *Theileria annulata* Ta9 protein contributes to activation of the AP-1 transcription factor, PLoS One 13 (2018) e0196875.

[36] F. Brühlmann, C. Perry, C. Griessen, K. Gunasekera, J.-L. Reymond, A. Naguleswaran, et al., TurboID mapping reveals the exportome of secreted intrinsically disordered proteins in the transforming parasite *Theileria annulata*, mBio 15 (2024) e03412.

[37] J.R. Stabel, T.J. Stabel, Immortalization and characterization of bovine peritoneal macrophages transfected with SV40 plasmid DNA, Vet. Immunol. Immunopathol. 45 (1995) 211–220.

[38] K. Elati, E. Zweygarth, M. Mhadhbi, M.A. Darghouth, A.M. Nijhof, Cultivation, cryopreservation and resuscitation of *Theileria annulata* transformed cells in serum-free media, Front. Vet. Sci. 9 (2022) 1055022.

[39] M.A. Bakheit, E. Endl, J.S. Ahmed, U. Seitzer, Purification of macroschizonts of a Sudanese isolate of *Theileria lestoquardi* (*T. lestoquardi* [Atbara]), Ann. N. Y. Acad. Sci. 1081 (2006) 453–462.

[40] S. Tajeri, D. Chattopadhyay, G. Langsley, A.M. Nijhof, A *Theileria annulata* parasite with a single mutation, methionine 128 to isoleucine (M128I), in cytochrome B is resistant to buparvaquone, PLoS One 19 (2024) e0299002.

[41] D. Kim, B. Langmead, S.L. Salzberg, HISAT: a fast spliced aligner with low memory requirements, Nat. Methods 12 (2015) 357–360.

[42] M. Pertea, G.M. Pertea, C.M. Antonescu, T.C. Chang, J.T. Mendell, S.L. Salzberg, StringTie enables improved reconstruction of a transcriptome from RNA-seq reads, Nat. Biotechnol. 33 (2015) 290–295.

[43] M.I. Love, W. Huber, S. Anders, Moderated estimation of fold change and dispersion for RNA-seq data with DESeq2, Genome Biol. 15 (2014) 550.

[44] M. Kanehisa, M. Araki, S. Goto, M. Hattori, M. Hirakawa, M. Itoh, et al., KEGG for linking genomes to life and the environment, Nucleic Acids Res. 36 (2008) D480–D484.

[45] X. Mao, T. Cai, J.G. Olyarchuk, L. Wei, Automated genome annotation and pathway identification using the KEGG Orthology (KO) as a controlled vocabulary, Bioinformatics 21 (2005) 3787–3793.

[46] M.D. Young, M.J. Wakefield, G.K. Smyth, A. Oshlack, Gene ontology analysis for RNA-seq: accounting for selection bias, Genome Biol. 11 (2010) R14.

[47] C. Zhang, Q. Shao, M. Liu, X. Wang, J.J. Loor, Q. Jiang, et al., Liver fibrosis is a common pathological change in the liver of dairy cows with fatty liver, J. Dairy Sci. 106 (2023) 2700–2715.

[48] K.J. Livak, T.D. Schmittgen, Analysis of relative gene expression data using real-time quantitative PCR and the 2(-Delta Delta C(T)) Method, Methods 25 (2001) 402–408.

[49] R. Lizundia, M. Chaussepied, M. Huerre, D. Werling, J.P. Di Santo, G. Langsley, c-Jun NH2-terminal kinase/c-Jun signaling promotes survival and metastasis of B lymphocytes transformed by *Theileria*, Cancer Res. 66 (2006) 6105–6110.

[50] N. Echebli, M. Mhadhbi, M. Chaussepied, C. Vayssettes, J.P. Di Santo, M. A. Darghouth, et al., Engineering attenuated virulence of a *Theileria annulata*–infected macrophage, PLoS Neglected Trop. Dis. 8 (2014) e3183.

[51] R.E. Adamson, F.R. Hall, Matrix metalloproteinases mediate the metastatic phenotype of *Theileria annulata*-transformed cells, Parasitology 113 (1996) 449–455.

[52] H.A. Baylis, A. Megson, R. Hall, Infection with *Theileria annulata* induces expression of matrix metalloproteinase 9 and transcription factor AP-1 in bovine leucocytes, Mol. Biochem. Parasitol. 69 (1995) 211–222.

[53] A.B. Keenan, D. Torre, A. Lachmann, A.K. Leong, M.L. Wojciechowicz, V. Utti, et al., ChEA3: transcription factor enrichment analysis by orthogonal omics integration, Nucleic Acids Res. 47 (2019) W212–w214.

[54] M. Chaussepied, N. Janski, M. Baumgartner, R. Lizundia, K. Jensen, W. Weir, et al., TGF-b2 induction regulates invasiveness of *Theileria*-transformed leukocytes and disease susceptibility, PLoS Pathog. 6 (2010) e1001197.

[55] D. Haller, M. Mackiewicz, S. Gerber, D. Beyer, B. Kullmann, I. Schneider, et al., Cytoplasmic sequestration of p53 promotes survival in leukocytes transformed by *Theileria*, Oncogene 29 (2010) 3079–3086.

[56] K. Hayashida, K. Kajino, M. Hattori, M. Wallace, I. Morrison, M.I. Greene, et al., MDM2 regulates a novel form of incomplete neoplastic transformation of *Theileria parva* infected lymphocytes, Exp. Mol. Pathol. 94 (2013) 228–238.

[57] M. Ngubo, F. Moradi, C.Y. Ito, W.L. Stanford, Tissue-specific tumour suppressor and oncogenic activities of the Polycomb-like protein MTF2, Genes 14 (2023).

[58] Z. Durrani, J. Kinnaird, C.W. Cheng, F. Brühlmann, P. Capewell, A. Jackson, et al., A parasite DNA binding protein with potential to influence disease susceptibility acts as an analogue of mammalian HMGA transcription factors, PLoS One 18 (2023) e0286526.

[59] Q. Zeng, J. He, X. Chen, Q. Yuan, L. Yin, Y. Liang, et al., Recent advances in hematopoietic cell kinase in cancer progression: mechanisms and inhibitors, Biomed. Pharmacother. 176 (2024) 116932.

[60] Y. Saito, H. Yuki, M. Kuratani, Y. Hashizume, S. Takagi, T. Honma, et al., A pyrrolo-pyrimidine derivative targets human primary AML stem cells in vivo, Sci. Transl. Med. 5 (2013) 181ra52.

[61] K. Elati, S. Tajeri, I. Obara, M. Mhadhbi, E. Zweygarth, M.A. Darghouth, et al., Dual RNA-seq to catalogue host and parasite gene expression changes associated with virulence of *T. annulata*-transformed bovine leukocytes: towards identification of attenuation biomarkers, Sci. Rep. 13 (2023) 18202.

[62] E. van der Heijden, L. Lefevre, A. Gossner, T. Tzelos, T.K. Connelley, M.A. Hassan, Comparative transcriptional analysis identifies genes associated with the attenuation of *Theileria parva* infected cells after long-term in vitro culture, Sci. Rep. 14 (2024) 8976.

[63] B.R. Shiels, S. McKellar, F. Katzer, K. Lyons, J. Kinnaird, C. Ward, et al., A *Theileria annulata* DNA binding protein localized to the host cell nucleus alters the phenotype of a bovine macrophage cell line, Eukaryot. Cell 3 (2004) 495.

[64] D.G. Swan, K. Phillips, A. Tait, B.R. Shiels, Evidence for localisation of a *Theileria* parasite AT hook DNA-binding protein to the nucleus of immortalised bovine host cells, Mol. Biochem. Parasitol. 101 (1999) 117–129.

[65] D.G. Swan, L. Stadler, E. Okan, M. Hoffs, F. Katzer, J. Kinnaird, et al., TashHN, a *Theileria annulata* encoded protein transported to the host nucleus displays an association with attenuation of parasite differentiation, Cell Microbiol. 5 (2003) 947–956.

[66] D.G. Swan, R. Stern, S. McKellar, K. Phillips, C.A.L. Oura, T.I. Karagenc, et al., Characterisation of a cluster of genes encoding *Theileria annulata* AT hook DNA-binding proteins and evidence for localisation to the host cell nucleus, J. Cell Sci. 114 (2001) 2747.

[67] J. Guergnon, M. Chaussepied, P. Sopp, R. Lizundia, M.-F. Moreau, B. Blumen, et al., A tumour necrosis factor alpha autocrine loop contributes to proliferation and nuclear factor-κB activation of *Theileria parva*-transformed B cells, Cell Microbiol. 5 (2003) 709–716.

[68] M. Ma, M. Baumgartner, Intracellular *Theileria annulata* promote invasive cell motility through kinase regulation of the host actin cytoskeleton, PLoS Pathog. 10 (2014) e1004003.

[69] M.A. Morris, C.W. Dawson, L.S. Young, Role of the Epstein-Barr virus-encoded latent membrane protein-1, LMP1, in the pathogenesis of nasopharyngeal carcinoma, Future Oncol. 5 (2009) 811–825.

[70] A.R.M. Almeida, J.L. Neto, A. Cachucho, M. Euzébio, X. Meng, R. Kim, et al., Interleukin-7 receptor α mutational activation can initiate precursor B-cell acute lymphoblastic leukemia, Nat. Commun. 12 (2021) 7268.
[71] C. Wang, L. Kong, S. Kim, S. Lee, S. Oh, S. Jo, et al., The role of IL-7 and IL-7R in cancer pathophysiology and immunotherapy, Int. J. Mol. Sci. 23 (2022).
[72] C. Cougoule, S. Carréno, J. Castandet, A. Labrousse, C. Astarie-Dequeker, R. Poincloux, et al., Activation of the lysosome-associated p61Hck isoform triggers the biogenesis of podosomes, Traffic 6 (2005) 682–694.
[73] C.A.L. Oura, S. McKellar, D.G. Swan, E. Okan, B.R. Shiels, Infection of bovine cells by the protozoan parasite *Theileria annulata* modulates expression of the ISGylation system, Cell Microbiol. 8 (2006) 276–288.
[74] X. Liu, J.G. Chen, M. Munshi, Z.R. Hunter, L. Xu, A. Kofides, et al., Expression of the prosurvival kinase HCK requires PAX5 and mutated MYD88 signaling in MYD88-driven B-cell lymphomas, Blood Adv 4 (2020) 141–153.
[75] B. Henry, L.D. Sibley, A. Rosenberg, A Combination of Four Nuclear Targeted Effectors Protects *Toxoplasma* against Interferon Gamma Driven Human Host Cell Death during Acute Infection, bioRxiv., 2023.
[76] J. Nyagwange, E. Awino, E. Tijhaar, N. Svitek, R. Pelle, V. Nene, Leveraging the Medicines for Malaria Venture malaria and pathogen boxes to discover chemical inhibitors of East Coast fever, Int J Parasitol Drugs Drug Resist 9 (2019) 80–86.
[77] S. Hacılarlıoglu, H.B. Bilgic, S. Bakırcı, A. Tait, W. Weir, B. Shiels, et al., Selection of genotypes harbouring mutations in the cytochrome b gene of *Theileria annulata* is associated with resistance to buparvaquone, PLoS One 18 (2023) e0279925.
[78] H. Sharifiyazdi, F. Namazi, A. Oryan, R. Shahriari, M. Razavi, Point mutations in the *Theileria annulata* cytochrome b gene is associated with buparvaquone treatment failure, Vet. Parasitol. 187 (2012) 431–435.
[79] M. Mhadhbi, M. Chaouch, K. Ajroud, M.A. Darghouth, S. BenAbderrazak, Sequence polymorphism of cytochrome b gene in *Theileria annulata* Tunisian Isolates and its association with buparvaquone treatment failure, PLoS One 10 (2015) e0129678.
[80] D. Tang, M. Chen, X. Huang, G. Zhang, L. Zeng, G. Zhang, et al., SRplot: a free online platform for data visualization and graphing, PLoS One 18 (2023) e0294236.